Highly Dipolar, Optically Nonlinear Adducts of Tetracyano-*p*-quinodimethane: Synthesis, Physical Characterization, and Theoretical Aspects

Marek Szablewski,[†] Philip R. Thomas,[†] Anna Thornton,[†] David Bloor,*[,†] Graham H. Cross,*[,†] Jacqueline M. Cole,[‡] Judith A. K. Howard,[‡] Massimo Malagoli,[§] Fabienne Meyers,[§,||] Jean-Luc Brédas,[§] Wim Wenseleers,[⊥] and Etienne Goovaerts[⊥]

Contribution from the Departments of Physics and Chemistry, University of Durham, Durham DH1 3LE, U.K., Service de Chimie des Materiaux Nouveaux, Université de Mons Hainaut, B-7000 Mons, Belgium, Physics Department, University of Antwerp-UIA, Universiteitsplein 1, B-2610 Antwerp, Belgium, and The Beckman Institute, California Institute of Technology, Pasadena, California 91125

Received November 12, 1996[⊗]

Abstract: A new series of nonlinear optical molecules are described where the ground state polarization is predominantly zwitterionic when the molecules are dissolved in solution. The molecules, which are derived in general from facile reactions between tertiary amines and tetracyano-*p*-quinodimethane (TCNQ), are of a type where the stabilization of the charge-separated ground state is favored by an increase in aromaticity over the neutral, quinoidal forms of the molecules. The measured second-order optical nonlinearity of one in the series has been measured by hyper-Rayleigh scattering and a figure of merit value, $\mu\beta(0)$, being the product of the dipole moment and static first hyperpolarizability, is found to be 9500×10^{-48} esu. This value, which is higher than most other reported values, is taken from studies in chlorinated solvents of relatively low polarity, but the discussion emphasizes the evolution of $\mu\beta(0)$ with solvent polarity, showing that even higher values could be expected with only modest increases in the polarity of the surrounding medium. The analysis of experimental data taken during dipole moment studies is thoroughly examined, and it is concluded that full account must be taken of the molecular shape to correlate the results with theoretical calculations. An ellipsoidal reaction field model is preferred for these highly one-dimensional molecules having strongly anisotropic polarizabilities.

Introduction

Nonlinear optical (NLO) phenomena underpin many of the operations performed by devices in telecommunications system switching nodes and provide a means for optical signal processing in general. Organic materials have now long been recognized as a potential alternative to inorganic glasses and semiconductors for device fabrication. Nonresonant optical nonlinearities are the highest among the organics where control over the optical nonlinearity has been approached through understanding the molecular structure/property relationships.[1−4] Much activity has concentrated on increasing the magnitude of the second-order molecular hyperpolarizability, β, in organic chromophores.[5−7] Those chromophores comprising an electron donor (D) linked to an electron acceptor (A) by means of a conjugated π electron system such as a benzene ring or polyene are classic examples, the simplest of which is *p*-nitroaniline. In such a system there is an asymmetry in the polarization of electrons within the π system leading to a dipole.

The degree to which the two resonance states of the molecule, one "neutral" and one charge separated or, zwitterionic, contribute to the ground state structure defines the polarization (i.e., $D-\pi-A$ to $D^+-\pi-A^-$). This is inevitably sensitive to the surrounding environment which acts to perturb the "vacuum" polarization. One of the simplest descriptions of environmental influences over dipole moment lies within Onsager's reaction field theory.[8,9] Here, the polarized medium surrounding the molecular dipole exerts a "reaction field" back onto the molecule and acts through its linear polarizability, α, to further enhance the dipole. More recently, interest has turned to the evolution of the higher molecular polarizabilities as a function of this reaction field.[10−13] The first hyperpolarizability, β, for example, in model polyenic systems displays both positive and negative

* Authors to whom correspondence should be addressed.
[†] Department of Physics, University of Durham.
[‡] Department of Chemistry, University of Durham.
[§] Université de Mons Hainaut.
[⊥] University of Antwerp-UIA.
[||] California Institute of Technology.
[⊗] Abstract published in *Advance ACS Abstracts,* March 1, 1997.

(1) Davydov, B. L.; Kotovshchikov, S. G.; Nefedov, V. A. *Sov. J. Quantum. Electron* **1977,** *7,* 129.
(2) Oudar, J. L. *J. Chem. Phys,* **1977**, *67,* 446. Williams, D. J. *Angew. Chem., Int. Ed. Engl.* **1984**, *23,* 690.
(3) Marder, S. R.; Gorman, C. B.; Meyers, F.; Perry, J. W.; Bourhill G.; Brédas J. L.; Pierce, B. M. *Science* **1994**, *265,* 632.
(4) Kanis, D. R.; Ratner, M. A.; Marks, T. A. *Chem. Rev.* **1994,** *94, 195.*
(5) Marder, S. R.; Cheng, L. T.; Tiemann, A. C.; Friedli, A. C.; Blanchard-Desce, M.; Perry, J. W.; Skindhøj, J. *Science* **1994,** *263,* 511.
(6) Laidlaw, W. M.; Denning, R. G.; Verbiest, T.; Chauchard, E.; Persoons, A. *Nature* **1993,** *363,* 58.
(7) Dhenaut, C.; Ledoux, I.; Samuel, I. D. W.; Zyss, J.; Bourgault, M.; LeBozec, H. *Nature* **1995,** *374,* 339.
(8) Onsager, L. *J. Am. Chem. Soc.* **1936,** *58,* 1486.
(9) Böttcher, C. J. F. *Theory of Electric Polarization*; Elsevier: Amsterdam, 1973, Vol. 1; 1978, Vol. 2.
(10) Marder, S. R.; Beratan, D. N.; Cheng, L. T. *Science* **1991**, *252,* 1030. Marder, S. R.; Perry, J. R.; Bourhill, G.; Gorman, C. B.; Tiemann, B. G.; Mansour, K. *Science* **1993,** *261,* 186.
(11) Dehu, C.; Meyers, F.; Hendrickx, E.; Clays, K.; Persoons, A.; Marder, S. R.; Brédas, J. L. *J. Am. Chem. Soc.* **1995,** *117,* 10127.
(12) Meyers, F.; Marder, S. R.; Pierce, B. M.; Brédas, J. L. *J. Am. Chem. Soc.* **1994,** *116,* 10703.
(13) Lu, D.; Chen, G.; Perry, J. W.; Goddard, W. A. *J. Am. Chem. Soc.* **1994**, *116,* 10679.

S0002-7863(96)03923-6 CCC: $14.00

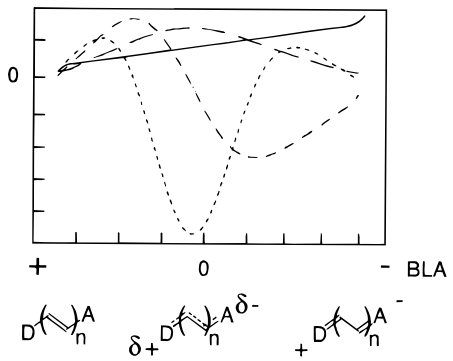

Figure 1. Evolution of the dipole moment, μ (solid line), and the molecular hyperpolarizabilities, α (large dashed), β (small dashed), and γ (dotted), with bond length alternation (BLA) of model donor−acceptor polyenes.

maxima when considered as a function of a polarizing field directed along the dipolar axis[3] (see Figure 1). The evolution of the hyperpolarizability reflects the changes in the electronic structure of the molecule as the field is applied. Theoretical and experimental studies of D−polyene−A systems[10,12] have thus emphasized the extent to which molecular structure affects the magnitude and sign of β. A convenient measure of the evolution of the π electron structure is given by the bond length alternation,[10] BLA (i.e., the average difference between the lengths of adjacent carbon−carbon double and single bonds along the polyene segment). When such a field is applied to a polar polyene structure, the geometry of the molecule undergoes a "cross-over" to a charge-separated "zwitterionic" structure. Initially the BLA is conventionally taken as positive, becoming zero at the "cyanine" limit: the point at which there is equivalent π electron density in the ground state and lowest charge transfer excited state. When the structure tends toward the charge-separated state the BLA becomes negative. The two maxima for $|\beta|$ occur on either side of the "cyanine" limit, a positive β, when BLA is positive, and a negative β when BLA is negative (Figure 1).

It has been found both theoretically and by experiment that different combinations of donors and acceptors with a wide range of conjugated "bridges" result in differing degrees of polarization and hence different magnitudes of β. Most synthesis programs in the field of organic materials for nonlinear optics have been targeted toward maximizing a positive β, yet it is clear that in, for example, merocyanine NLO molecules, stabilization of the charge-separated state is relatively easy to achieve.[14] Merocyanines in this form are extremely susceptible to protonation however which removes their optical nonlinearity.[15] The merocyanines achieve this zwitterionic state largely because there is an increase in aromaticity to be gained from charge separation. In most other molecules studied for nonlinear optics this feature is not available or not particularly favored. In a recent report of some tricyanoquinodimethane (TCQ) molecules,[16] related to those which we report herein, the ground state structure is still predominantly quinoid-like (see, for example, structure **12**, Figure 2). In this particular compound, however, it is suggested that due to polarization effects the first maximum in β has been passed. The solution state dipole moments measured in chloroform were not exceptional however (around 12−13 D) which indicates that the structures are not strongly polarized even here.

Stabilization of a charge-separated state may be achieved at a sufficiently high reaction field, i.e. in polar environments. The dielectric theory indicates that reaction fields are highest when the solute dipole moment and polarizability and the solvent dielectric constant are all high. The dipole moment which a solute molecule therefore has in solution depends on these factors but also, and significantly, on the stabilization energies involved in separating charge. In favorable circumstances, molecules in solution will display all the characteristics of the polarization responses described on the right-hand side (RHS) of the BLA diagram. Henceforth therefore we will distinguish such molecules as RHS types. The merocyanines are such species while the TCQ derivatives of ref 16 may not be. Experimentally one might easily identify RHS molecules by virtue of their negative solvatochromic behavior.[17] The position of the charge transfer band in the UV/visible absorption spectrum moves to shorter wavelengths with an increase in solvent polarity. Incidentally, such molecules will also have considerably enhanced dipole moments in these media over LHS (left-hand side) molecules.

Among the few RHS NLO molecules reported to date are the merocyanine dyes[14] (structure **9**, Figure 2), heterocyclic betaines[18] (structure **10**, Figure 2), and a molecule comprising an imidazolidine TCNQ adduct[19] (DCNQI) (structure **11**, Figure 2). Metzger[20] reported the synthesis and X-ray crystallographic structure of a TCQ−pyridinium species (structure **13**, Figure 2) with a high degree of charge separation in the crystal environment. Here a calculated value for the dipole moment was reported to be 26 D, obtained by a closed-shell INDO calculation using the crystallographic geometry. Second-harmonic generation was observed by Ashwell[21] in Langmuir−Blodgett films of the related amphiphilic pyridinium, quinolinium, and benzthiazolium[22] (structures **14**−**16,** Figure 2) analogues. A negative solvatochromic shift was noted in these materials. One other TCNQ-derived zwitterionic adduct (as indicated by crystal structure) has been reported in which the donor and acceptor are linked by a σ bond (structure **17**, Figure 2).[23]

The high electron affinity of the TCQ acceptor and the highly dipolar nature of adducts containing this group has prompted a number of theoretical modeling investigations. Honeybourne,[24] for example, reported calculations on pyridinium−TCQ species stressing the negative sign of β and the dipole moment *decrease* on excitation to the first excited state (i.e., negative $\Delta\mu$). More recently Broo and Zerner[25,26] investigated the nature of the ground state structure of **13** (Figure 2) and the effects of environment on the ground state properties and absorption spectra. It was concluded that the geometry of the species in liquid solution reflects intermediate BLA, whereas in the crystal form, the bond-alternated zwitterionic form predominates. Our

(14) Fort, A.; Runser, C.; Barzoukas, C.; Combellas, C.; Suba, C.; Thiebault, A. *Proc. SPIE.* **1984,** *2285,* 5.
(15) Girling, I. R.; Kolinsky, P. V.; Cade, N. A.; Earls, J. D.; Peterson, I. R. *Optics. Commun.* **1985,** *55,* 289.
(16) Boldt, P.; Bourhill, B.; Branchle, C.; Yiwen, J.; Kammler, R.; Müller, C.; Rase, J.; Wichern, J. *J. Chem. Soc., Chem. Commun.* **1996,** 793.
(17) Brooker, L. G. S.; Keyes, G. H.; Heseltine, D. W. *J. Am. Chem. Soc.* **1951,** *73,* 5350.
(18) Alcalde, E.; Roca, T.; Redondo, J.; Ros, B.; Serrano, J. L.; Rozas, I. *J. Org. Chem.* **1994,** *59,* 644.
(19) Lalama, S. J.; Singer, K. D.; Garito, A. F.; Desai, K. N. *Appl. Phys. Lett.* **1981,** *39,* 940.
(20) Metzger, R. M.; Heimer, N. E.; Ashwell, G. J. *Mol. Cryst. Liq. Cryst.* **1984,** *107,* 133.
(21) Ashwell, G. J.; Dawnay, E. J. C.; Kuczyński, A. P.; Szablewski, M.; Sandy, I. M.; Bryce, M. R.; Grainger, A. M.; Hasan, M. *J. Chem. Soc., Faraday Trans.* **1990,** *86,* 1117.
(22) Ashwell, G. J.; Malhotra, M.; Bryce, M. R.; Grainger, A. M. *Synth. Met.* **1991,** *43,* 3173.
(23) Miller, J. S.; Calabrese, J. C. *J. Chem. Soc., Chem. Commun.* **1988,** 63.
(24) Honeybourne, C. L. *J. Phys. D.: Appl. Phys.* **1990,** *23,* 245.
(25) Broo, A.; Zerner, M. C. *Chem. Phys.* **1995,** *196,* 407.
(26) Broo, A.; Zerner, M. C. *Chem. Phys.* **1995,** *196,* 423.
(27) Cole, J. C.; Cole, J. M.; Howard, J. A. K.; Cross, G. H.; Szablewski, M.; Farsari, M. *Acta Crystallogr., Sect. B,* in press.

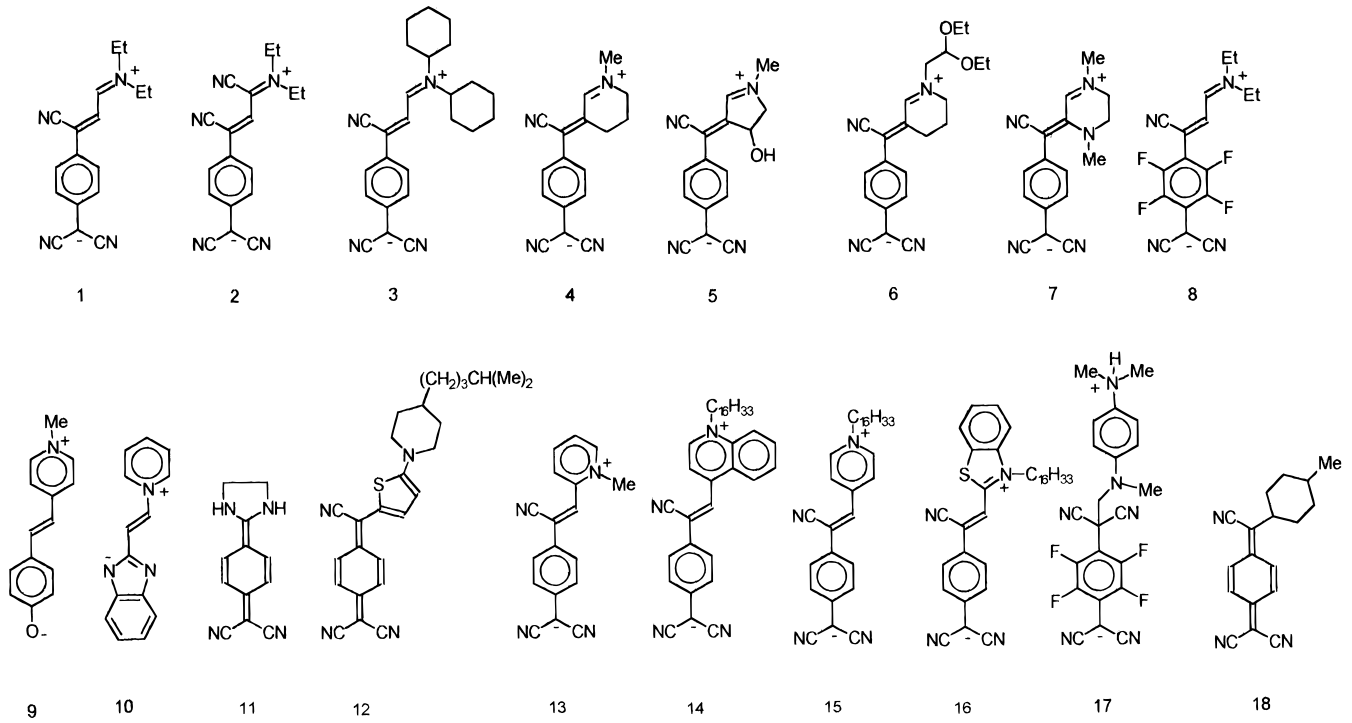

Figure 2. Chemical structures of compounds referred to in the text.

own observations[27] confirm that, in molecules of this type, crystal field effects stabilize the charge-separated structure.

RHS Molecules Formed from Tertiary Amines and TCNQ. As a result of our discovery of a novel reaction of TCNQ with triethylamine[28] which led to the synthesis of DEMI (structure **1**, Figure 2), we have prepared a range of similar adducts of TCNQ with tertiary ethylamines (structures **1**−**8**). All of these adducts have similar π electron systems, a TCQ acceptor separated from an electron-deficient amino moiety. The spectral properties of these species are therefore very similar, comprising a broad charge transfer band in the middle of the visible region with very little absorption to either side of it. The low optical absorption between 400 and 500 nm prompted us to describe these molecules as "blue window" chromophores.[29,30]

The synthetic procedure used to synthesize the analogues (**1**−**8**, Figure 2) involves the direct reaction to TCNQ of a tertiary amine derivative, such as triethylamine,[28] in which at least one of the substituent groups is an ethyl moiety. We initially reported the synthesis of DEMI (**1**) to be carried out in chloroform, but have since found that the preferred solvent of choice is chlorobenzene, a higher boiling point solvent which allows the reactions to reach completion in a matter of hours rather than 3 days as previously reported.[28] The reaction proceeds *via* the formation of an enamine which subsequently attacks the TCNQ in a Stork enamine-type reaction. The critical step therefore in the synthetic procedure is the formation of the enamine. The reactivity depends on the degree of stabilization of the enamine by functionalities adjacent to the site of its formation in the tertiary amine. We developed a phenomenological model of reactivity which suggested that electron-withdrawing groups adjacent to the amino functionality discourage enamine formation by decreasing the electron density on the amino nitrogen. This principle is clearly illustrated by the failure to react of (electron-withdrawing) fluorinated and (diphenylamino)ethyl tertiary amines with TCNQ.

Although the nonlinear and linear optical properties calculated and determined experimentally[31,32] for **1** are favorable in view of applications, there are several significant difficulties which have to be overcome in order to make such materials viable options for use in nonlinear optical devices, namely solubility, stability to photo-oxidation, and hydration. The planarity and high dipole moment encourages aggregation while the presence of ethylenic bonds and a strong optical transition can sensitize singlet oxygen formation leading to photo-oxidation.[33] The thermal stability of **1** has been investigated by differential scanning calorimetry, and decomposition occurs at 243 °C in air. This is similar to other TCQ-type chromophores which have recently been reported.[16]

The nonlinearity of the DEMI chromophore is extremely high, and it is therefore desirable to limit changes to the molecular architecture to those which will not decrease this property when attempting to synthesize variants. As the core of the molecule's nonlinearity lies in its conjugated backbone linking the quaternized nitrogen to the negatively charged dicyanovinylidene, significant changes cannot be made to this part of the molecule. However either the replacement of the third nitrile group or substitutions on either the aromatic ring of the acceptor or on two of the "arms" of the tertiary amine donor can be tolerated. The aromatic/quinoidal ring is critical in maintaining a charge-separated state, the stability associated with an aromatic moiety playing an important part in determining the geometry of the molecule. The extent to which this effect influences the nonlinearity and polarity can be seen by comparing **1** to adducts of TCNE (tetracyanoethylene),[34] which are molecules containing the tricyanovinyl acceptor group. These molecules are pre-

(28) Szablewski, M. *J. Org. Chem.* **1994,** *59,* 954.
(29) Cole, J. C.; Howard, J. A. K.; Cross, G. H.; Szablewski, M. *Acta Crystallogr., Sect. C* **1995,** *C51,* 715.
(30) Cross, G. H.; Bloor, D.; Szablewski, M. *Nonlinear Opt.* **1995,** *14,* 219.
(31) Ranjel-Rojo, R.; Kar, A. K.; Wherret, B. S.; Carroll, M.; Cross, G. H.; Bloor, D. *Rev. Mex. Fis.* **1995,** *41,* 832.
(32) Healy, D.; Thomas, P. R.; Szablewski, M.; Cross, G. H. *Proc. SPIE* **1995,** *2527,* 32.
(33) Prein, M.; Adam, W. *Angew. Chem., Int. Ed. Engl.* **1996,** *35,* 477.
(34) Katz, H. E.; Singer, K. D.; Sohn, J. E.; Dirk, C. W.; King, L. A.; Gordon, H. M. *J. Am. Chem. Soc.* **1987,** *109,* 6561.

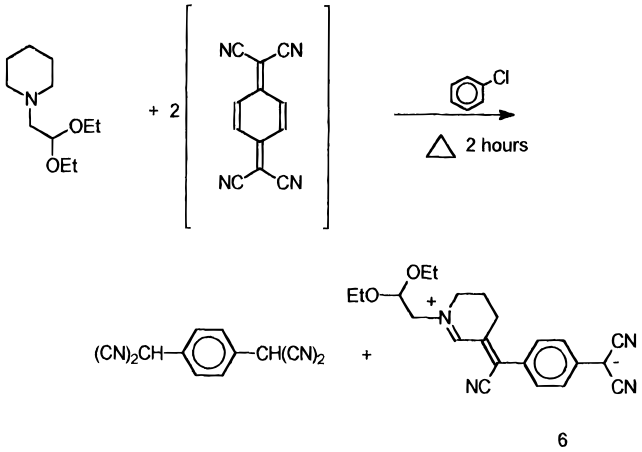

Figure 3. Reaction scheme for the synthesis of **6**.

Table 1. Limiting Solubilities (mol/L) Determined by Adherence to Beer−Lambert Law Behavior for a Selection of Chromophores

chromophore	acetonitrile	chlorobenzene
1	2×10^{-4}	5×10^{-5}
3	9×10^{-4}	2×10^{-4}
4	7×10^{-4}	3×10^{-5}
6	9×10^{-3}	2×10^{-3}

dominantly non-charge-separated and reside on the left-hand side (LHS) of the BLA diagrams.

As ether groups are known to aid solubility we thus replaced one nitrile group at one end of the TCNQ with a methoxide group.[35] Reactions were carried out using diethylamine. In both cases these TCQ derivatives, on further reaction with triethylamine, resulted simply in **1**, the amino or ethoxide group proving more labile than the remaining nitrile.

Tertiary amine piperidines were used to produce ring-closed systems (structures **4, 5,** and **7**, Figure 2). Computer modeling showed a reduced planarity along the conjugated bridge yet no significant changes in solubility were observed. Nevertheless, these "ring-closed" derivatives proved more inert to hydration in hygroscopic solvents (such as DMF), thus making their handling in such high-polarity solvents much easier.

A significantly more soluble material (**6**) was synthesized by the reaction of 1-piperidineacetaldehyde diethyl acetal with TCNQ. Some solubilities were determined and are shown in Table 1.

The use of hydroxy groups on five- and six-membered saturated N-heterocyclic systems, i.e. 3-hydroxy-1-methylpiperidine, provided a starting point for further functionalization. The hydroxy functionalities were converted to benzyl ethers and *tert*-butyl benzyl ethers; however, subsequent reactions with TCNQ were unsuccessful. The predominant products were, in both cases, TCNQ radical anion salts.

Solid State Structure

The charge-separated ground state has been confirmed by crystallographic structural studies[29] of **1** (Figure 4, structure **1**). The ring system has been found to be predominantly quinoidal rather than aromatic (Table 2), although the backbone is conjugated from the nominally "positive" nitrogen to the "negative" carbon; carbon−carbon double bonds are lengthened while carbon−carbon single bonds are shortened. Charges are assigned on the basis of the shortening of the C13−N4 bond to 1.316 Å and the fact that all the bond angles around N4 are between 117.4 and 122.6°. The negative charge is considered to be delocalized over the dicyanomethanide unit and into the ring. Such assignments do however emphasize the inadequacy of using conventional Kekulé structures to represent such species. We have found[27] that the presence of the residual bridge cyano group is necessary for the retention of quinoidal character. The extra nitrile group in **2** extends the conjugated system with respect to the otherwise isostructural **1**, resulting in a molecule which is more quinoidal.

Quantum-Chemical Calculations. There is a growing interest in applying computational techniques which in some way account for solute environment.[11,36−39] The COSMO continuum dielectric model,[38] for example, calculates reaction fields using solvent dielectric constant, ϵ_s, and solute radii as parameters. Studies on a series of conventional D−π−A molecules[39] assuming solvation in DMSO ($\epsilon_s = 45$) show that modest increases in dipole moment can be expected.

No such assumptions are involved in the following analysis which simply applies a field to the molecule without regard to its likely origin. The influence of the effective field at the molecule is studied at the semiempirical INDO (intermediate neglect of differential overlap) level. Fields are applied in the direction favoring charge separation along the molecular dipole moment axis. Molecular geometries in the presence of the field have been optimized at the SCF (self-consistent field) level, and calculations of the dipole moment, μ, polarizability tensor, α, and dipole-directed first hyperpolarizability component, β, have been performed by means of the sum-over-states (SOS) formalism (40 states) on the basis of state energies, state dipole moments, and transition moments computed with a single excitation configuration interaction (SCI) calculation.[40] Calculations based on the simple two-state model using the lowest energy charge transfer state were also made. Figure 5 shows the evolution of μ and β for **1** as a function of the effective local field. In the absence of externally applied fields, this is simply the effective *reaction* field of the polarizable dipole in its polarizable surroundings. The field strengths used are in the range 0.002−0.02 au which correspond to 10^7-10^8 V/cm.[41] Increasing the strength of the electric field transforms the geometry of DEMI from neutral to zwitterionic. Of particular interest is the prediction that even in the absence of a reaction field (gas phase) the molecule has a structure where the first maximum in β has been passed. Even so, in the gas phase, **1** starts on the left-hand side of the polyene model diagram but rapidly crosses over into the right-hand side at only modest reaction fields.

Interestingly, the solid state geometry (in the crystal) of **1** can be reproduced using these methods by applying a field of 0.008 au. This implies that the molecular dipole moment in the crystal is around 35 D (referring to Figure 5).

(35) Acker , D. S.; Blomstrom, D. C. U.S. Patent 3,115,506, 1963.

(36) Barzoukas, M.; Fort, A.; Boy, P.; Combellas, C.; Thiebault, A. *Nonlinear Optics* **1994**, *7*, 41.

(37) Albert, I. D. L.; di Bella, S.; Kanis, D. R.; Marks, T. J.; Ratner, M. A. Polymers for second-order nonlinear optics. *ACS Symp. Ser*. **1995**, *601*, 57.

(38) Klamt, A.; Schüürmann, G. *J. Chem. Soc., Perkin Trans. 2* **1993**, 799.

(39) Allin, S. B.; Leslie, T. M.; Lumpkin, R. S. *Chem. Mater*. **1996**, *8*, 428.

(40) The β value calculated from the 40-state model is expected to be very close to the converged value. In the case of the *p*-nitroaniline, we have previously analyzed the dependence of the polarizabilities as a function of the number of excited states included in the SOS expression. We found a fast convergence of the second-order response (within a 10% error) after only 30 states. (See: Ramasesha S.; Shuai Z.; Brédas, J. L. *Chem. Phys. Lett*. **1995**, *245*, 224.)

(41) Conversion factor: 1 au = 5.14192×10^{11} V m^{-1}.

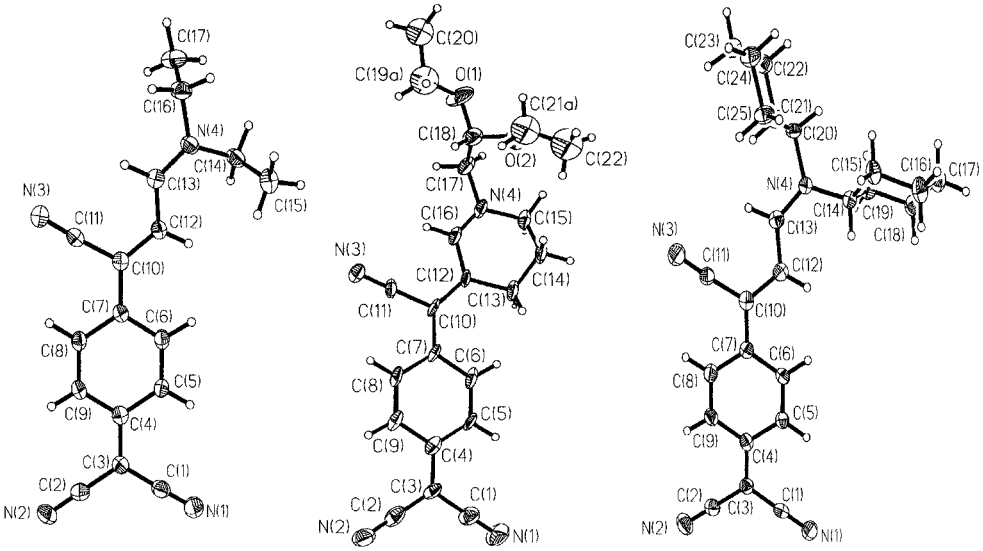

1 3 6

Figure 4. X-ray crystal structures of compounds[29] **1**, **3**, and **6**.

Table 2. Carbon−Carbon Bond Distances (Å) for Compounds **3** and **6** Taken from the X-ray Crystal Structures (150 K)

C*n*−C*m*	**3**	**6**
C4−C5	1.422(4)	1.41(1)
C5−C6	1.370(5)	1.36(1)
C6−C7	1.415(5)	1.437(9)
C7−C8	1.418(5)	1.41(1)
C8−C9	1.368(5)	1.36(1)
C4−C9	1.412(5)	1.434(9)

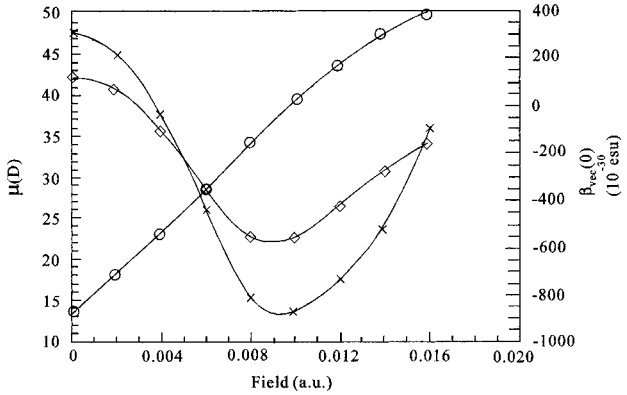

Figure 5. Evolution versus perturbing field of the ground state polarization components μ (circles) and $\beta(0)$ for **1**, calculated using a 40-state SOS model (diamonds). Also shown for $\beta(0)$ are the computed values using the two-state model (crosses).

Solvatochromism

The electronic (visible absorption) spectra of all the "zwitterionic" species reported above are characterized by a broad band in the region 650−750 nm, with areas of transparency either side of the main peak. The majority of adducts have a spectrum similar to that of **1** (Figure 6), where the major band consists (in the case of **1** in dichloromethane) of two major peaks at (approximately) 720 nm (A) and 657 nm (B) with two shoulders at 615 nm (C) and 550 nm (D).

While band B displays only a small positive solvatochromism, band A displays marked *negative* solvatochromism over a given range of solvent environments. The solvatochromism of band

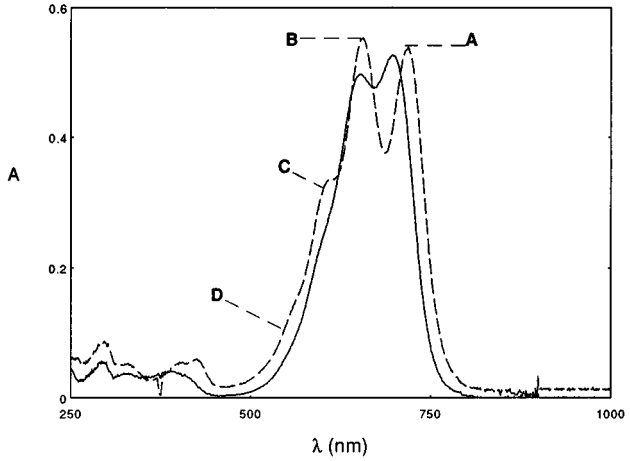

Figure 6. UV/vis spectrum of compound **1** in acetonitrile (solid line) and dichloromethane (dotted line) with labelled peaks.

A in the spectra of some of the compounds is given as a function of solvent dielectric constant in Table 3. Note that the monosubstituted amine TCQ species (structure **18**, Figure 2) is included for comparison since this species does not exhibit any noticeable negative solvatochromism and is thus clearly a LHS molecule. In the remainder of the compounds, the initial decrease in transition energy minimizes in chlorobenzene and then increases in the more polar solvents. Anomalies appear in the general trend; for example, protic solvents such as alcohols tend to cause a much greater hypsochromic shift than expected.

It is worth mentioning that the fluorinated analogue of **1** (structure **8**) exhibits a dramatic shift of −58 nm for peak A in comparison to the spectral properties of **1** in acetonitrile. This suggests that the extra electron-withdrawing moieties on the TCQ part of the molecule hamper the back charge-transfer from A^- to D^+, thus shifting the band to a higher energy. This trend is consistent with the effect of applying a larger electric field to the molecule. Here the higher reaction field caused by the (presumably) larger dipole in **8** is responsible.

Further evidence of the increase in zwitterionic character of DEMI analogues in increasingly polar media can be obtained from ^{1}H NMR solvatochromic studies of the more soluble

Table 3. Position (nm) of the Lowest Energy Excitation (Band A) versus Solvent Dielectric Constant, ϵ, for a Selection of Compounds Referred to in the Text

		compound no.								
solvent	ϵ	**1**	**2**	**3**	**4**	**5**	**6**	**7**	**8**	**18**
1,4-diox.	2.2	711		720	712	716	719	604		
benzene	2.3	708					720			571
toluene	2.4	702		716	724		718	648		
$(Et)_2O$	4.3	701		716	710		715			559
$CHCl_3$	4.8	717	721	726	719	722	721	624	725	
PhCl	5.6	722	725	728	722	726	727	672	730	571
THF	7.6	719		723	708	723	718	667	704	
DCM	8.9	720	723	725	719	722	718	653	716	570
C_6H_{10}=O	16.1	715	785	723	701		710	667		584
$(Me)_2CO$	20.7	705		712	688	707	697	655	653	565
TM-urea	23.1	708		717	689	709	698	653		
EtOH	24.6	703		709	671	703	678			
MeOH	32.7	688		700	652	693	658		622	
CH_3NO_2	35.9	702		708	664		686	646	649	582
DMF	36.7	693	802	708	665	697	679	656		
MeCN	37.5	698	785	705	680	702	680	643	640	565
DMSO	46.7	670		702	662	668	667	652		574

Chart 1

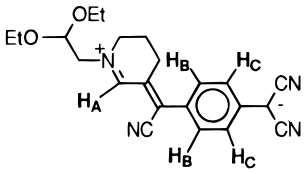

compound **6**. The high sensitivity of the NMR technique in detecting subtle changes in electron density in molecular structures makes it valuable for investigations of this type.[14] Chart 1 gives the structure of **6** again but with relevant protons identified and indicated on the NMR spectrum of **6** in Figure 7.

The protons experiencing the largest changes in shielding due to shifting π electron density will be H_A adjacent to the developing positive charge on the amino nitrogen. The next most sensitive would be the two aromatic/quinoid ring protons, (H_C), closest to the developing negative charge on the dicyanomethanide group; these are seen as a doublet at lowest field in the fragment of the spectrum considered (Figure 7). The other doublet H_B seen in the spectrum represents the two remaining ring protons. Proton NMR spectra of **6** were recorded in deuterated analogues of chloroform, dichloromethane, acetone, DMSO, and MeCN, and all were measured relative to the scale TMS = 0 ppm.

We would expect the signal observed for proton H_A to shift to higher field as it is increasingly deshielded by the depletion of charge on the nitrogen. This is indeed what is seen in progressively more polar solvents (using the dielectric constant as a simple index for solvent polarity). The developing negative charge on the dicyanomethanide group would be expected to increasingly shield the ring protons H_C with increasing solvent polarity. Such a trend is clearly seen. It is interesting to note that protons H_B shift slightly *downfield*, apparently more influenced by the formation of the positive charge rather than the negative charge.

Solution Dipole Moment Measurements and Underlying Theoretical Principles. A coaxial capacitance cell was used to measure the dielectric constant of dilute solutions of compound **1** at 1 MHz. Low solubility prevented the use of strictly nonpolar solvents as usually required, but acceptable results have been obtained using dichloromethane as solvent. Concentrations of around 10^{-4} mol dm^{-3} were typical. Such

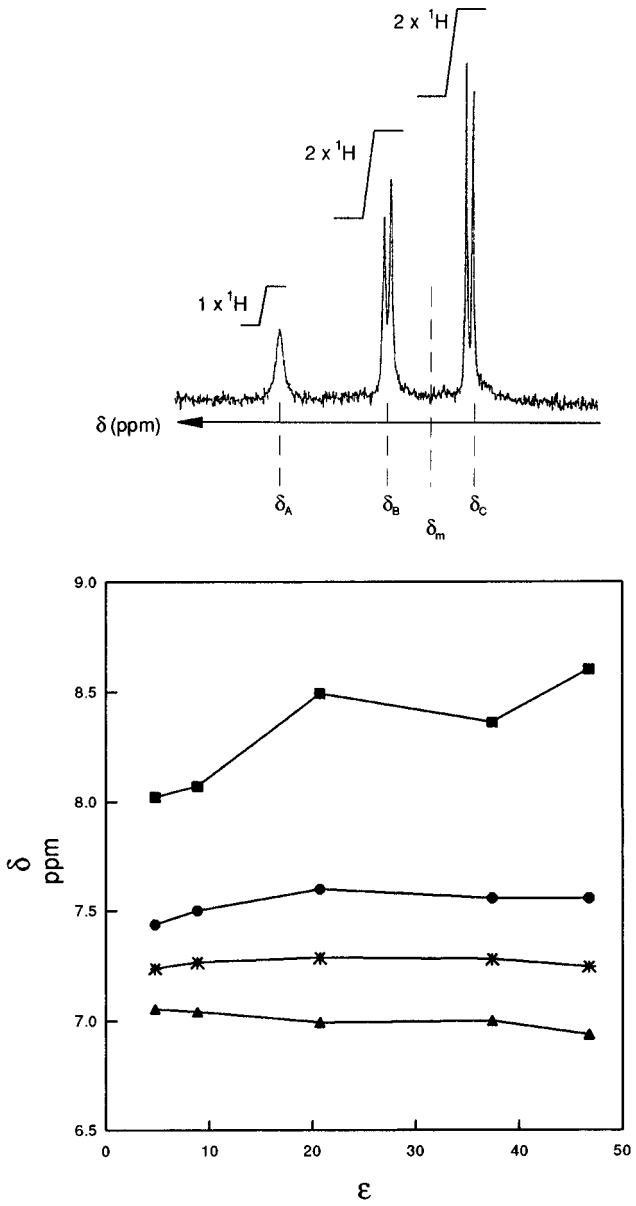

Figure 7. Top: ^{1}H NMR of compound **6**; typical splitting pattern for ethylenic and aromatic protons H_A, H_B, and H_C, referred to in the text. Bottom: The chemical shift of ethylenic and aromatic protons taken from the ^{1}H NMR spectrum of compound **6** versus solvent dielectric constant. Singlet δ_A, doublet δ_B, doublet δ_C, and the midpoint of the two doublets, δ_m, are represented by squares, circles, triangles, and stars, respectively.

low solubilities have prevented us from using the conventional techniques (density studies) to determine the volume of the solute molecules and their effective radii. In addition, due to the absorbance over much of the visible region, refractive index measurements (to yield solute polarizabilities) are further complicated. We are currently exploring methods to determine the near-infrared refractive indices of solutions.

There have been a number of methodologies for analysing the data from experiments of this nature, but we prefer that which was outlined by Myers and Birge[42] as the basis for our own analysis. Here the molecules are treated as polarizable ellipsoidal particles when considering the directing field acting on the dipoles. For the induced dipolar contributions, however, a spherical model is satisfactory and in any case the induced dipoles are considerably smaller than the permanent dipoles whose reorientation dominates the dielectric constant.

(42) Myers, A. B.; Birge, R. R. *J. Chem. Phys.* **1981,** *74,* 3514.

In a polarized solution containing a polarizable dipolar solute the total polarization per unit volume, $\vec{P}_{tot}$, may be given by

$$\vec{P}_{tot} = \vec{P}_s + \vec{P}_m \quad (1)$$

where $\vec{P}_s$ is the polarization contribution from the solvent and $\vec{P}_m$ is the total contribution from the dipolar solute. The total dipolar polarization is further considered to be resolvable into those contributions arising from induced dipoles, $\vec{P}_\alpha$, and orienting permanent moments, $\vec{P}_\mu$, as follows:

$$\vec{P}_m = \vec{P}_\alpha + \vec{P}_\mu \quad (2)$$

We immediately state that, in the initial analysis, the dipole moment, μ, is that which already benefits from enhancement through the reaction field its ground state moment (μ_0) produces. Thus the analysis which follows will yield *solution state* dipole moments.

According to standard methods assuming an isotropic dipole distribution and low applied electric fields (as in these measurements), we have

$$\vec{P}_\mu = N_m \frac{\mu^2}{3kT} \vec{E}_r \quad (3)$$

where N_m is the number density of dipolar particles and $\vec{E}_r$ is the "directing field". In the case of polarizable ellipsoidal particles (with semiaxes labeled *a*, *b*, and *c*), the directing field may be related to the applied field, $\vec{E}$, by taking account of the cavity field factor (obtained from solving Laplace's equation for vacuum cavities in a dielectric medium), G_{ell} and the additional applied field-induced reaction field due to the polarizability of the particle. Thus we follow the method of Böttcher[9] and represent the total directing field as

$$\vec{E}_r = F_{ell} G_{ell} \vec{E} = \frac{1}{(1 - f_a \alpha_a)} \frac{\epsilon_s}{\epsilon_s + (1 - \epsilon_s) A_a} \vec{E} \quad (4)$$

where F_{ell} is the ellipsoidal reaction field correction factor which depends upon the factor of the reaction field, f_a, along the dipolar axis, *a*, in the molecule whose polarizability along this axis is α_a. The surrounding dielectric constant, ϵ_s, is, in our analysis, that of the pure solvent. Before proceeding, we are careful to point out that the dielectric constant used here should strictly be that of the *solution* but in using this constant value we simplify the analysis without sacrificing accuracy. Our justification lies in the fact that we use only very dilute solutions and thus observe only rather small changes to the measured dielectric constant of solutions over these ranges of concentration.

The ellipsoid shape factor,[9] A_a, may be calculated from the following:

$$A_a = \frac{abc}{2} \int_0^\infty \frac{ds}{(s + a^2)^{3/2} (s + b^2)^{1/2} (s + c^2)^{1/2}} \quad (5)$$

and is readily determined using commercial mathematics software (e.g., "Mathematica" [43]).

The factor of the reaction field, f_a, is given by

$$f_a = \frac{3}{\bar{a}^3} \frac{A_a (1 - A_a)(\epsilon_s - 1)}{\epsilon_s + (1 - \epsilon_s) A_a} \quad (6)$$

where $\bar{a}$ is the radius of a notional sphere occupying the same volume as the ellipsoidal dipole. This parameter is particularly difficult to define since it should properly represent the distance from the central point dipole to the point at which the boundary conditions are applied in solving Laplace's equation. In Onsager's theory, the boundary of the cavity is a discontinuity in the permittivity, but other arbitrary conditions may be chosen to acheive the unique solution to Laplace's equation. For example, Block and Walker[44] allow the permittivity to grow exponentially (from unity) to the bulk value outside the defining radius and indeed claim better agreement between gas phase and liquid dipole moment values. In the following analysis, two physical limits to the radius are defined: first, that which may be obtained from the density values obtained from the crystal structure and, second, that which is represented by the quantity $(abc)^{1/3}$. Other than these limits, the radius will be treated as a parameter to be determined so that it can include the unknown properties of the solute/solvent boundary.

We need to determine the ellipsoidal shape factor, A_a, and thus (from eq 5) to determine reasonable values for the semiaxes *a*, *b*, and *c*. Using a commercial molecular modeling package (Nemesis[45]) we have modeled compound **1** and calculated the solvent accessible surface using a probe radius of 1.5 Å (as an estimate of the radius of a dichloromethane molecule). Using this we measure the shortest distances between pairs of surface contact points along the length, width, and thickness of the molecular surface to yield $a = 7.6$ Å, $b = 3.4$ Å, and $c = 1.9$ Å. Solving eq 5 gives $A_a = 0.106$.

The induced dipole contribution, $\vec{P}_\alpha$, is considered to be represented very well by the action of the applied field on a "spherical" particle having an average polarizability, $\bar{\alpha}$. This assumption has been made before[42] with success and, although we are describing considerably more elongated molecules than those previously, is valid here simply because this contribution is very much smaller than $\vec{P}_\mu$.

The induced polarization is given by

$$\vec{P}_\alpha = N_m \bar{\alpha} \vec{E}_i \quad (7)$$

where we use the average polarizability, $\bar{\alpha} = (\alpha_a + \alpha_b + \alpha_c)/3$, and the internal field, $\vec{E}_i$, is given by

$$\vec{E}_i = F_{sph} G_{sph} \vec{E} = \frac{1}{(1 - f_{sph} \bar{\alpha})} \frac{3\epsilon_s}{2\epsilon_s + 1} \vec{E} \quad (8)$$

where F_{sph} and G_{sph} are the spherical model counterparts of the reaction field factor and cavity field factor described above. The spherical model factor of the reaction field, f_{sph}, is given by

$$f_{sph} = \frac{1}{\bar{a}^3} \frac{2\epsilon_s - 2}{2\epsilon_s + 1} \quad (9)$$

By noting the definition for induced polarization, $\vec{P} = \epsilon_0(\epsilon - 1)\vec{E}$, we can make the approximation for the solvent polarization contribution such that

$$\vec{P}_s = \epsilon_0(\epsilon_s - 1)\vec{E} \quad (10)$$

This polarization is taken to be approximately constant over the solution concentration ranges used and is measured from the pure solvent capacitance value. This yields the solvent dielectric constant contribution to the solution dielectric constant, ϵ, and after making substitutions into eq 1 we obtain

(43) Mathematica v 2.1, Wolfram Research Inc.

(44) Block, H.; Walker, S. M. *Chem. Phys. Lett.* **1973**, *19*, 363.

(45) Nemesis v 2.0, Oxford Molecular Ltd.

$$\epsilon = \epsilon_s + N_m\left[F_{sph}G_{sph}\bar{\alpha} + F_{ell}G_{ell}\frac{\mu^2}{3kT}\right] \qquad (11)$$

Differentiating with respect to solute number density and rearranging (11) gives a convenient formula for calculating the solution state dipole moment:

$$\mu = \left\{\left[\left.\frac{\partial\epsilon}{\partial N_m}\right|_0 - F_{sph}G_{sph}\bar{\alpha}\right]\frac{3kT}{F_{ell}G_{ell}\epsilon_0}\right\}^{1/2} \qquad (12)$$

where μ is in MKSA units if the experimental slope is provided in units of m^3. The number density used here is the value obtained from the molar concentration of solute and assumes that changes in the density of solution with concentration are negligible when compared with changes in dielectric constant.[46] This is valid at the concentration of these experiments and constitutes no more than a 2% error on experimental values.[47] We note that for typical values of average polarizability the second term in parentheses will often be orders of magnitude smaller than the slope value. Whilst neglecting this term will marginally simplify the determination of μ, there is no extra benefit in reducing the inherent uncertainties in estimating either molecular dimensions or polarizabilities.

At room temperature, we measured the solvent dielectric constant (dichloromethane) to be 8.6 ($\pm$0.8), which is close to the quoted textbook value[48] of 8.9. This value was used as the constant solvent contribution to the dielectric constant. The only parameter for which a measurement has not been obtained is the polarizability. Values of both the average polarizability and the polarizability along the dipole axis are required.

Measurements of refractive index of solutions can yield the average polarizability from which the *a* axis component can be obtained,[9] but suitably chosen molecular dimensions are again required. However, Myers and Birge have suggested[42] that it is better to use the actual value for α_a if it is available. Here we use the calculated zero field values for molecule **1** obtained from the INDO calculations outlined above. Thus we use $\alpha_a = 121 \times 10^{-30}$ m^3, $\alpha_b = 12 \times 10^{-30}$ m^3, and due to the planarity, $\alpha_c = 0$. Therefore the average polarizability $\bar{\alpha} = 44 \times 10^{-30}$ m^3.

Using this data and our experimental slope value, we can determine the solution state dipole moments where the average solute radius is the unknown variable. In parameterizing the radius we are exploring the possible reaction fields implied from our experimental data. Despite the experimental results relying on particular values for α_a and $\bar{\alpha}$ obtained theoretically, the preferred *radius* (which is the quantity of least certainty) would be defined when there was self-consistent agreement between the experimental solution state moment and theoretical data at a common value of field. Thus we show a plot of these dipole moments versus field in Figure 8. The solution state dipole moments are obtained using eq 12 but where the field factors are parameterized using a range of $\bar{a}$. The reaction field is obtained from the following:

$$R_{ell} = \frac{f_a}{(1 - f_a\alpha_a)}\mu_0 \qquad (13)$$

but noting that $\mu_0 = (1 - f_a\alpha_a)\mu$ which gives

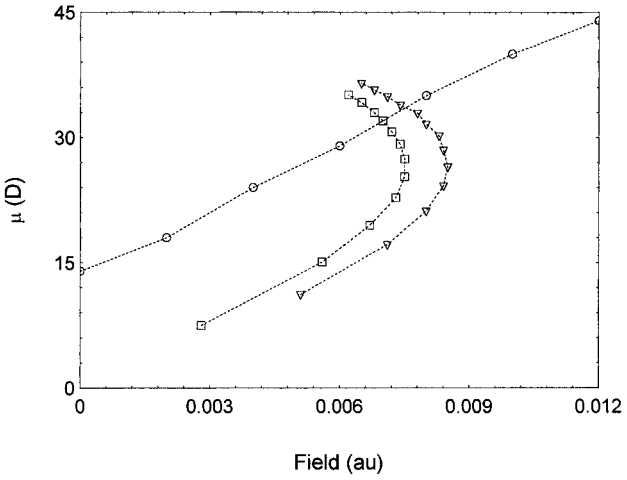

Figure 8. Dipole moments of **1** obtained by experiment plotted as a function of reaction field, both obtained using average solute radius as a parameter. Reaction field values are computed using eq 14 for a range of solute average radii. Experimental moments and fields using the INDO calculated gas phase polarizabilities (triangles) and first-order corrected values (squares) are shown. The theoretical dipole moment evolution versus field is also provided (circles).

$$R_{ell} = f_a\mu \qquad (14)$$

The experimental solution state dipole moment crosses the theoretical curve when $\mu = 33.2 \pm 2.5$ D and when $R_{ell} = 0.0077$ au. The gas phase dipole moment can be calculated for the specific value of f_a using the value for α_a given above. This yields $\mu_0 = 17.1$ D. The value of the solute average radius which corresponds to this data is 4.13 Å, which is larger than the average radius obtained from the cube root of the products of *a*, *b*, and *c* (3.66 Å) yet smaller than that determined from the crystal structure density data (4.43 Å). We would not wish to apply any particular physical definition for this radius but simply note that it lies within reasonable physical limits.

The INDO calculated gas phase value is 14 D, and this indicates that there is a small overestimation in the experimental dipole moment and reaction field values calculated using the above parameters. There are two possible reasons for this. First, the values of polarizability assumed are the gas phase values yet we have calculated an evolution in these parameters with field. Thus better estimates of dipole moment would use these (higher) values which are more relevant to experimental conditions. Second, this discrepancy could be due to the Kirkwood "solvent cage" effect.[49] Dichloromethane is a slightly polar solvent, and we might expect an enhancement to the reaction field from this effect.

As a first-order correction to these results, we can use the INDO calculated values of α_a and $\bar{\alpha}$ versus field and re-compute the experimental data as a function of solute radius. Using the gas phase values for μ_0 and α_a in eq 13, we obtain a field of 0.0062 au at which the calculated evolved values for α_a and $\bar{\alpha}$ are 137 and 50 $\times 10^{-30}$ m^3, respectively. The experimental data obtained for these values is also shown in Figure 8. Here the crossing point occurs at $R = 0.0071$ au, where $\mu = 31.3 \pm 2.4$ D and $\mu_0 = 14.1$ D. Clearly this is in rather better agreement with the theoretical data.

It is of interest to compare the spherical model theory when applied to the experimental results. Here we find that an average radius of 4.2 Å would be required to give the INDO gas phase moment. However, using the spherical model for this radius

(46) Scholte, Th. G. *Recueil* **1951,** *70,* 50.
(47) Singer, K. D. University of Pennsylvania Ph.D. Thesis, 1981.
(48) Riddick, J. A.; Bunger, W. B.; Sakano, T. K. *Organic Solvents, Physical properties and methods of purification,* 4th ed.; John Wiley and Son Inc.: New York, 1986.
(49) See, for example: Frölich, H. *Theory of Dielectrics*; Oxford Science Publications: Oxford, U.K., 1986.

and with the average polarizability $\bar{\alpha} = 44 \times 10^{-30}$ m^3 and $\mu_0 = 14$ D, the reaction field value becomes $R_{sph} = 0.018$ au (using an equation analogous to eq 13). This is clearly unrealistic and serves to reinforce the argument for careful use of the ellipsoidal field theory.

Finally, despite the apparent success in its use, we acknowledge that this analysis places heavy reliance on the quality of quantum-chemical calculations. Measurements of density (and therefore of the average radius of the solute-occupied volume) coupled with solute refractive index measurements in an appropriate spectral region are still to be preferred, where these are possible.

Measurements of First Hyperpolarizability, β. The measurement of $\mu\beta$ by the usual EFISHG (electric field induced SHG) method using 1.064 μm radiation turns out to be difficult for these molecules due to the finite optical absorption at 532 nm and to problems of aggregation at the concentrations suitable for this measuring technique. This problem was circumvented by the application of the hyper-Rayleigh scattering (HRS) technique, in which lower concentrations can be employed because the signal is linear with concentration (instead of quadratic as for EFISHG).[50]

HRS measurements with a fundamental wavelength at 1.064 μm were performed on dilute solutions (number density, $1-2.6 \times 10^{16}$ cm^{-3}) of **1** in chloroform. The solutions were systematically passed through 500 nm microporous filters. Laser pulses (energy, 20−25 μJ; width, 70 ps; repetition rate, 2 kHz) from a Nd:YAG regenerative amplifier were focused into a rectangular glass cell by a 10 cm lens. The scattered harmonic light was collected at 90° and filtered by a monochromator with 1 nm bandwidth. Single-photon pulses from a photomultiplier were detected in a 5 ns time gate around the laser pulse. The count rates were corrected for pile-up errors at increasing count rates and for absorption (<5%) of the scattered light. Systematic scanning of a narrow region around 532 nm showed no significant photoluminescence background for solutions of **1** in these circumstances. In a reference arm, a fraction of the laser light was frequency-doubled and this intensity was used to correct for slow laser fluctuations.

Polarized measurements with analyzer perpendicular and parallel to the laser polarization, corrected for the relative monochromator transmission, show a ratio of $\langle\beta_{XZZ}^2\rangle/\langle\beta_{ZZZ}^2\rangle = 0.21 \pm 0.01$, which agrees, within experimental accuracy, with that of a molecule with only one non-zero diagonal tensor component, β_{zzz}. Note that the use of upper case subscripts denotes laboratory coordinates, and lower case, molecular coordinates. This ratio is to be expected for this compound with its linear conjugated backbone. Using the internal reference method we obtained a ratio $\beta_{HRS}/[\beta_{HRS}(CHCl_3)]$ of 1600 (where β_{HRS} stands for $[\langle\beta_{ZZZ}^2\rangle + \langle\beta_{XZZ}^2\rangle]^{1/2}$). Applying the previously used approximation[50] that the β-tensor of chloroform is also dominated by β_{zzz} and adopting the EFISH value for β_{CHCl_3} of 0.49×10^{-30} esu,[51] the measured near-resonance value of $\beta(-2\omega;\omega,\omega)$ in this approximation is $|\beta_{ZZZ}| = 780 \pm 25 \times 10^{-30}$ esu. The usual spherical local field models were applied in this analysis, and we are thus able to compare the present results with other published work.

We can turn to the reaction field model and compare this resonant value with that predicted and shown in Figure 5. For chloroform ($\epsilon_s = 4.8$), we calculate (from eq 13) $R_{ell} = 0.0058$ au, using $\mu_0 = 14.1$ D, $\alpha_a = 137 \times 10^{-30}$ m^3, and $\bar{a} = 4.13$ Å. At this value of field we see from the INDO results that $\beta(0) = (-320 \pm 50) \times 10^{-30}$ esu. Since the 40-state SOS model results are, fortuitously, nearly equivalent to the simple two-level model results at this value of reaction field, we can use the two-level correction factor, F_β:

$$F_\beta = \frac{{\omega_0}^4}{[{\omega_0}^2 - \omega^2][{\omega_0}^2 - (2\omega)^2]} \qquad (15)$$

where ω_0 and ω are the frequency of the lowest energy optical transition (here λ_{max} in $CHCl_3 = 717$ nm) and the experimental frequency, respectively, to determine that the experimental $|\beta(0)| \approx (350 \pm 11) \times 10^{-30}$ esu. This is in excellent agreement with theory.

The solution state dipole moment of **1** has not been measured in chloroform (due to solubility difficulties), but we can assume that the theoretical predicted value of 27 D in a field of 0.0058 au is a good approximation in view of the foregoing. We can therefore report that, in $CHCl_3$, the molecular figure of merit, $\mu\beta(0)$, for **1** is 9450×10^{-48} esu.[52]

Conclusions

Tertiary amine adducts of TCNQ prepared by a simple one-step facile reaction exhibit a charge-separated ground state structure indicated by their negative solvatochromism. These materials are expected to show higher figures of merit for second-order optical nonlinearity, $\mu\beta(0)$, than LHS molecules, not especially because of their high hyperpolarizability, but because of the inevitably high dipole moments when in solution. The polarization properties of the adducts evolve with increasing solvent polarity, and we have observed that all of them quickly become what we have termed RHS molecules, being on the right-hand side of the cyanine limit in diagrams depicting bond length alternation versus polarization. The increasing dipole moment has been confirmed from shifts in the ^{1}H NMR spectra as a function of solvent polarity. Measurements of the polarization properties have required close attention to the properties of the local field description. Particularly where static directing fields are concerned, as in the dipole moment measurements, we show in some detail that it is essential to consider the molecules as ellipsoidal volumes in the surrounding continuum rather than as notional spherical volumes. Detailed theoretical calculations of the ground state polarization properties as a function of perturbing field only agree with experimental data when account is taken of the molecular shape. The value for the moment in dichloromethane of one in the series is 31 D and its expected value in chloroform reduces to 27 D. The measured value for the static hyperpolarizability measured by hyper-Rayleigh scattering in chloroform is 350×10^{-30} esu, giving one of the highest reported values for $\mu\beta(0)$. We note that, with only a slight increase in reaction field, this value could, based on the quantum-chemical calculations, be increased to around $17\,500 \times 10^{-48}$ esu. Problems in confirming this exceptional nonlinearity are related to those of interpreting dipole moment measurement data taken from studies using highly dipolar solvents. Furthermore, the utility of these materials relies on their being hosted in solid polymeric matrices where the reaction fields are not expected to be high. Measurements of the dipole moment of these molecules in polymer films is continuing and will be reported on separately.[53]

(50) Clays, K.; Persoons, A. *Phys. Rev. Letts.* **1991,** *66, 2980.*
(51) Kajzar, F.; Ledoux, I.; Zyss, J. *Phys. Rev. A* **1987**, *36*, 2210.
(52) Some authors prefer to take account of the volume-normalized figure-of-merit by simply dividing by molecular weight. On this basis, we can quote a value for compound **1** of $9450 \times 10^{-48}/276$ esu g^{-1} mol.
(53) Cross, G. H.; Healy, D.; Szablewski, M.; Bloor, D.; Malagoli, M.; Kogej, T.; Beljonne, D.; Brédas, J.-L. *Chem. Phys. Lett.* **1997**, in press.

Chart 2

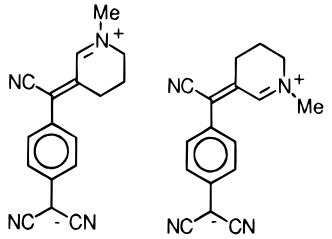

Experimental Section

General Procedure for Preparation of Dipolar TCNQ Adducts. A solution of TCNQ (2 mol equiv) in chlorobenzene was heated under reflux for 0.5 h. Tertiary amine (1 mol equiv) in chlorobenzene solution was added dropwise. The reaction mixture was heated at reflux from 3 h up to 60 h dependent on the tertiary amine used. The reaction solution was monitored at intervals by UV/vis spectroscopy. When no TCNQ or $TCNQ^-$ peaks were seen and the characteristic "blue" band[26] was observed, the now blue/turquoise solution was removed from the heat. Filtration of the reaction mixture yielded a blue solution and a black residue. The solution was reduced to dryness under vacuum giving the crude product, more of which was obtained by extraction of the residue with acetonitrile.

The combined crude solids were recrystallized from acetonitrile three times to yield the product. The product was filtered under suction and washed with toluene and ether.

1. DEMI-3CNQ (4-[1-Cyano-3-(diethylamino)-2-propenylidene]-2,5-cyclohexadiene-1-ylidenepropanedinitrile). TCNQ (0.98 mmol, 2 mol equiv) and triethylamine (0.49 mmol, 1 mol equiv) refluxed for 4 h gave **1,** metallic-like green-gold needle-like crystals (990 mg) in 73% yield. ^{1}H NMR (DMSO-d_6): δ 0.8 ppm [quintet, $-(CH_3)_2$, δ 3.8 ppm, quintet, $-(CH_2)_2-$, δ 6.9 and 7.8 ppm, doublet of doublets, *p*-substituted benzene ring, δ 7.3 ppm doublet, ethylenic proton] δ 8.3 ppm [doublet, ethylenic proton nearest positively charged N]. Mass spectrum: *m/z* 276 (M^+) (100%, molecular ion). Decomposition temperature: 243.28 °C. IR (KBr disc): $\nu_{(\text{nitrile})}$ 2185.7, 2155.6 cm^{-1} (characteristic of C≡N stretch in such zwitterionic species), 1588.1 cm^{-1} (C═N str). Microanalysis. Calcd for $C_{17}H_{16}N_4$: C, 73.89; N, 20.27; H, 5.84%. Found: C, 73.78; N, 20.41; H, 5.76%. The structure of **1** was confirmed by X-ray crystallography; see ref 29.

2. CN-DEMI-3CNQ (4-[1,3-Dicyano-3-(diethylamino)-2-propenylidene]-2,5-cyclohexadiene-1-ylidenepropanedinitrile). 2 was the unexpected result of a preparation of **1** that was refluxed for an excessive period. TCNQ (0.49 mmol, 2 mol equiv) and triethylamine (0.24 mmol, 1 mol equiv) refluxed for 18 h gave **2,** dark green crystals (59 mg) in 8.15% yield. IR (KBr disc): $\nu_{(\text{nitrile})}$ 2199.61 cm^{-1} with small shoulder at approximately 2001 cm^{-1}. The small quantity of product did not allow an adequate microanalysis to be obtained. The structure of **2** was confirmed by X-ray crystallography; see ref 27.

3. Dicyclohexyl-DEMI-3CNQ (4-[1-Cyano-3-(dicyclohexylamino)-2-propenylidene]-2,5-cyclohexadiene-1-ylidenepropanedinitrile). TCNQ (0.98 mmol, 2 equiv) and dicyclohexylethylamine (0.49 mmol, 1 equiv) refluxed for 5 h gave **3**, metallic-like dark green-gold needle-like crystals (1130 mg) in 62% yield. ^{1}H NMR could not be recorded due to the highly insoluble nature of **3**. IR (KBr disc): $\nu_{(\text{nitrile})}$ 2188.49, 2160.58. cm^{-1}. Microanalysis. Calcd for $C_{25}H_{28}N_4$: C, 78.09; N, 14.57; H, 7.34%. Found: C, 77.74; N, 14.60; H, 7.27%. The structure of **3** was confirmed by X-ray crystallography; see attached structure and data.

4. (*N*-Methylpiperidyl)-DEMI-3CNQ. TCNQ (0.98 mmol, 2 mol equiv) and 1-methylpiperidine (0.49 mmol, 1 mol equiv) refluxed for 5 h gave **4,** metallic-like green-gold powder (428 mg) in 31.8% yield. ^{1}H NMR (DMSO) identified two isomers, A (60%) and B (40%) (assigned structures shown in Chart 2). These two species could not be separated by column chromatography. For species A: δ 2.00 ppm [triplet, ring $-(CH_2)-$ (nearest C═C bridge)], δ 2.9 ppm [triplet, ring $-(CH_2)-$ (adjacent to N^+)], δ 3.78 ppm [singlet, CH_3], δ 3.8 ppm [multiplet, ring $-(CH_2)-$ (β to ring N)], δ 6.9 ppm [doublet, 2 × aromatic ^{1}H (adjacent to dicyanomethanide)], δ 7.6 ppm [doublet, 2 × aromatic ^{1}H (adjacent to ethylenic bridge)], δ 8.8 ppm [singlet (ethylenic proton nearest positively charged N)]. For species B: δ 2.15 ppm [triplet, ring $-(CH_2)-$ (nearest C═C bridge)], δ 2.83 ppm [triplet, ring $-(CH_2)-$ (adjacent to N^+)], δ 3.74 ppm [singlet CH_3 δ 3.8 ppm, multiplet, ring $-(CH_2)-$ (β to ring N)], δ 6.9 ppm [doublet, 2 × aromatic ^{1}H (adjacent to dicyanomethanide)], δ 7.4 ppm [doublet, 2 × aromatic^{1}H (adjacent to ethylenic bridge)], δ 8.6 ppm [singlet, (ethylenic proton nearest positively charged N)]. IR (KBr disc): $\nu_{(\text{nitrile})}$ 2188.7, 2161.6 cm^{-1}. Microanalysis. Calcd for $C_{17}H_{14}N_4$: C, 74.43; N, 20.42; H, 5.14%. Found: C, 74.08; N, 20.37; H, 5.10%.

Chart 3

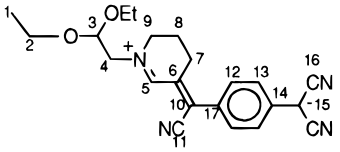

5. (*N*-Methyl-2-pyrolidinol)-DEMI-3CNQ. TCNQ (0.49 mmol, 2 mol equiv) and 1-methyl-3-pyrolidinol (0.24 mmol, 1 mol equiv) refluxed for 6 h gave **5** a dark green powder (150 mg) in 22.6% yield. Due to the highly insoluble nature of **5** a poor-quality ^{1}H NMR in CD_3-CN was obtained, it showed features in common with the other analogues described herein, namely: δ 7.0 and 7.65 ppm [doublet of doublets, *p*-substituted benzene ring], δ 8.2 ppm [ethylenic proton, δ 3.85 ppm, (OH)]. Mass spectrum: *m/z* (FABHI) 277.09 (3.81%) (M^+ + 1). IR (KBr disc): $\nu_{(\text{nitrile})}$ 2186, 2153.4 cm^{-1}, $\nu_{(\text{OH str.})}$ 3416 cm^{-1}. UV/vis spectra were consistent with other compounds described herein.

6. *N*-Acetaldehyde Diethyl Acetal-Piperidyl-DEMI-3CNQ. TCNQ (0.98 mmol, 2 equiv) and 1-piperidineacetaldehyde diethyl acetal (0.49 mmol, 1 equiv) gave **6**, lustrous emerald green platelets (540 mg) in 25% yield. **6** was recrystallized from hot acetonitrile, and a trace of an orange TCNQ decomposition product (λ_{max} = 480 nm in MeCN) was found to be present. Column chromatography performed on neutral silica gel with 1:9 acetonitrile:ethyl acetate eluent was used to purify the product. The purified compound was again recrystallized from acetonitrile. Crystals grown for X-ray structural determinations were obtained by slow recrystallization from hot dichloromethane. The data obtained indicated that one molecule of dichloromethane was present for every molecule of **6** in the crystal. ^{1}H NMR (CD_2Cl_2): δ 1.23 ppm [triplet, (2 × CH_3)], δ 2.02 ppm [quintet ($-CH_2-$)], δ 2.79 ppm [triplet ($-CH_2-$)], δ 3.5−3.8 ppm [multiplet [triplet ($-CH_2-$) + doublet ($-CH_2-$) + quartet 2 × ($-CH_2-$)]], δ 4.70 ppm [triplet ($-CH-$)]. δ = 7.02 ppm, doublet 2 × (−aromatic H−)], δ 7.49 ppm [doublet 2 × (−aromatic H−)], δ 8.08 ppm [singlet ($-N^+$═CH)]. ^{13}C NMR (see numbered structure in Chart 3): C1, δ 15.8 ppm; C2, δ 51.3 ppm; C3, δ 100.8 ppm; C4, δ 61.8 ppm; C5, δ 129.5 ppm; C6, δ 119.9 ppm; C7, δ 25.9 ppm; C8, δ 21.49 ppm; C9, δ 64.9 ppm; C10, δ 125.5 ppm; C11, δ 116.2 ppm; C12, δ 121.8 ppm; C13, δ 133.9 ppm; C14, δ 158.9 ppm; C16, δ 119.3 ppm; C17, δ 153.2 ppm. No peak was assigned for C15. IR (KBr disc): $\nu_{(\text{nitrile})}$ 2181.2, 2146.8 cm^{-1}. Microanalysis. Calcd for $C_{22}H_{24}N_4O_2$ (recrystallized from acetonitrile): C, 70.19; N, 14.88; H, 6.43%. Found: C, 69.85; N, 14.93; H, 6.19%.The structure of **6** was confirmed by X-ray crystallography; see attached structural data.

7. (*N*,*N*-Dimethylpiperazinyl)-DEMI-3CNQ. TCNQ (0.98 mmol, 2 mol equiv) and 1,4-dimethylpiperazine (0.49 mmol, 1 mol equiv) was heated at ∼105 °C for 60 h. **7** was collected in the form of green crystals. These were found not to be of analytical purity, however, the material was sufficiently soluble to obtain meaningful NMR data. Yield: 60 mg (42%). IR (KBr disc): $\nu_{(\text{nitrile})}$ 2190, 2160 cm^{-1}, $\nu_{(\text{imine})}$ 1598 cm^{-1}. ^{1}H NMR (DMSO-d_6): δ 2.05 ppm [singlet, 2H; δ 2.85 ppm, singlet, 2H; δ 3.4 ppm, singlet (broad), 6H], δ 6.90 ppm [doublet, 2H; δ 7.70 ppm, doublet, 2H: δ 8.00 ppm, singlet, 1H]. ^{13}C NMR (see Chart 4) (assigned with the aid of a 2D heteronuclear ^{13}C−^{1}H correlation spectrum): δ 30.7 ppm, C3; δ 42.1 ppm, C2; δ 49.0 ppm, C4; δ 68.6 ppm, C1; δ 115.3 ppm, C5; δ 115.8 ppm, C7; δ 115.9 ppm, C8; δ 119.3 ppm, C10; δ 119.9 ppm, C14; δ 129.5 ppm, C6; δ 130.9 ppm, C11; δ 131.8 ppm, C9; δ 152.4 ppm, C12; δ 166.7 ppm, C13. Microanalysis. Calcd for $C_{17}H_{15}N_5$: C, 70.6; N, 24.2; H, 5.2. Found: C, 67.0; N, 26.8; H, 3.9.

Chart 4

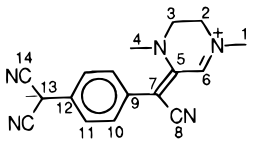

8. Tetrafluoro-DEMI-3CNQ (4-[1-Cyano-3-(diethylamino)-2-propenylidene]-2,3,5,6,-tetrafluoro-2,5-cyclohexadiene-1-ylidenepropanedinitrile). $TCNQF_4$ (0.036 mmol, 2 mol equiv) and triethylamine (0.018 mmol, 1 mol equiv) refluxed for 4 h gave **8,** a purple powder (27 mg, 21% yield). Very poor ^{1}H NMR (CD_3CN): δ 1.35 ppm [quintet, $-(CH_3)_2$, δ 3.85 ppm, quintet, $-(CH_2)_2-$, δ 8.4 and 7.2 ppm very weak signals, ethylenic ^{1}H]. ^{19}F NMR spectra in CD_2Cl_2 showed three singlets at δ −146.9, −137.8, and −136.3 ppm, integration in the ratio of 1:1:1.3; a ^{19}F NMR spectra of $TCNQF_4$ showed only one singlet at δ −132.2 ppm. UV/vis absorption spectra were in accordance with other analogues described above and displayed the characteristic bands expected; no $TCNQF_4$ or $TCNQF_4^-$ bands were observed in these spectra; the origin of the third singlet in the ^{19}F NMR spectra of **8** is unexpected and could possibly be due to the species $TCNQF_4H_2$.

18. 7-(4-Methylpiperidino)-7,8,8-tricyanoquinodimethane.[35] To a warm solution of TCNQ (0.49 mmol) in 100 cm^3 of tetrahydrofuran was added 0.6 cm^3 of 4-methylpiperidine. The initially green solution became purple. After being cooled overnight to room temperature, the solution was cooled in an ice bath and filtered to give a fine purple solid. Recrystallization from acetonitrile yielded fine purple needles, 531 mg (39% yield). ^{1}H NMR (DMSO-d_6): δ 0.08 ppm [doublet quintet, $-CH_3$], δ 0.65, 1.00, 2.95 and 3.40 ppm [multiplets (integration 2, 3, 2, and 2 × ^{1}H, respectively), aliphatic piperidine ring protons], δ 6.1 and 6.6 ppm [doublet of doublets, *p*-substituted quinoidal ring]. IR (KBr disc): $\nu_{(\text{nitrile})}$ 2188.7, 2161.6 cm^{-1}.Microanalysis: calculated for $C_{17}H_{16}N_4$: C, 73.89; N, 20.27; H, 5.84%. Found: C, 73.83; N, 20.30; H, 5.81%. The structure of **18** was confirmed by X-ray crystallography, see ref 27.

Acknowledgment. We thank the U.K. E.P.S.R.C. for support for M.S., A.T., J.M.C., and P.R.T. J.M.C. also receives support from the Institut Laue-Langevin (Grenoble, France). This work was also supported by funds provided under the EU Human Capital and Mobility Programme, Research Network, "Novel third-order nonlinear optical molecular materials" [CHRX-CT93-0334 (DG XII)]. The work in Mons is part funded by the Belgian Federal Government, "Pôle d'Attraction Interuniversitaire en Chimie Supramoleculaire et Catalyse", FNRS/FRFC, and an IBM Joint Study. We acknowledge the assistance given in NMR studies by Dr. R. S. Matthews. IR spectra were carried out by Mr. Y. Kagawa. The work in Antwerp is part funded by the Flanders Government in its action for the promotion of participation in EU-research programmes and also by the Belgian Fund for Scientific Research (F.W.O.).

Supporting Information Available: Details of instrumentation, reagents, and X-ray crystal structure determinations of **3** and **6** (18 pages). See any current masthead page for ordering and Internet access instructions.

JA963923W